Progress In Electromagnetics Research C, Vol. 49, 67–77, 2014

Analysis and Design of Millimeter-Wave Circularly Polarized Substrate Integrated Travelling-Wave Antennas

Halim Boutayeb* **and Ke Wu**

Abstract—Circularly polarized millimeter-wave travelling-wave antennas, using substrate integrated circuits (SICs) technology, are designed, fabricated and tested. By using the SICs technology, compact antennas with low losses in the feeding structure and with good design accuracy are obtained. The elementary antenna which is composed of two inclined slots is characterized by full-wave simulations. This characterization is used for the design and development of linear antenna arrays with above 16 dB gain and low side lobe level (< -25 dB), using different power aperture distributions, namely uniform, Tchebychev and Taylor. Experimental results are presented at 77 GHz showing that the proposed antennas present good performances in terms of impedance matching, gain and axial ratio. These antennas have potential applications in integrated transceivers for communication and radar systems at millimeter-wave frequencies.

1. INTRODUCTION

Using millimeter-wave (mm-wave) frequencies has important advantages including broad bandwidth and high data rate, small antenna size with high directivity, and good spectral/angular resolution, depending on their applications. There are several frequency bands in the mm-wave range which have been approved by the Federal Communications Commission (FCC) for wireless communications and automotive radar [1–4]. The 77-GHz band has been allocated for automotive radar, but it can be used for other applications such as short-range surveillance, microwave imaging, and ultra-high-speed data transmission.

The communication industries have been witnessing enormous growth in the field of wireless local area networks (WLAN). In the quest for more available bandwidth, much attention is paid to millimeter-wave frequencies. In particular, the unlicensed band at 60 GHz is of special interest, because of the high atmospheric attenuation due to oxygen absorption of 10 to 15 dB per km, which makes it unsuitable for long range communication (> 1 km) but suitable for short range communications, where radio cells are better defined and small, as inter-channel interference is less so that frequencies can be reused more often [5].

Low-cost and high-performance technologies are critical for communication in the mm-wave band. The Substrate Integrated Circuits (SICs) present a platform where all passive and active elements of a complete system can be integrated on a single substrate with the same processing technique [6]. Such integration is achieved with the use of discrete metallic via and air hole arrays to simulate equivalent electrical walls for designing, for example, substrate integrated waveguides (SIW), couplers, filters and antennas on a substrate [7–12]. Nowadays, this technique is largely studied and developed by researchers around the world.

With the use of the SICs technique, a radar front-end system at 24 GHz was designed and fabricated in [13] and a 24 GHz integrated multifunctional platform which capable of time-agile operations between

Received 30 January 2014, Accepted 8 April 2014, Scheduled 14 April 2014

* Corresponding author: Halim Boutayeb (h.boutayeb@polymtl.ca).

The authors are with the Ecole Polytechnique de Montréal, 2500 Ch. de Polytechnique, Pav. Lassonde, Montréal, Québec, H3T 1J4, Canada.

radio communications and radar modes has been presented in [14]. These integrated systems can be improved by optimizing the transmitting and receiving antennas. Since in these works, the two antennas are linearly polarized, the receiving power is dependent on the position of the system and therefore the isolation between the two antennas can become bad if the antennas are close to each other. Another drawback is that for the uniform standing wave slot array, the side lobes level cannot be less than −13 dB. Finally, the standing wave array used in [13] leads generally to narrow frequency bandwidth.

Circularly polarized antennas are particularly interesting for communication and radar systems. Besides that there is no need for the antenna's orientation as they also reduce considerably the multipath fading and thus increase the spectral efficiency of RF systems. In addition, when receiving and transmitting antennas are used with circular polarization, the isolation between the two antennas can be maximized. Furthermore, travelling-wave antenna arrays often lead to wider frequency bandwidth than standing wave or leaky wave counterparts. It should also be noted that these antennas are based on a design method which permits complete control of the main beam's orientation, gain and side lobe levels. In this contribution, we propose a complete analyze and design procedure for new circularly polarized substrate integrated travelling-wave antenna arrays operating at 60 GHz and 77 GHz, completing our previous work [15]. Linearly polarized SIW travelling-wave antennas have been presented in [16, 17]. In [18], travelling-wave circularly polarized SIW antennas have been proposed at 16 GHz by using double pairs of slots. In this work, a single pair of slots inspired by the radiation unit proposed in [19, 20] for rectangular waveguides is used for developing new SIW travelling wave antennas.

The remainder of the paper is organized as follows: Section 2 provides the characterization of circularly polarized antenna element using double inclined slots. The synthesis procedure of linear traveling-wave antennas is presented in Section 2. Sections 3 and 4 present the design techniques for the SIW and transitions. Sections 5 and 6 present numerical and experimental results and compare the performances of different arrays. It is shown that a good agreement is obtained between simulated and measured data. Finally, concluding remarks are given in Section 7.

2. CHARACTERIZATION OF AN ELEMENT OF THE ARRAY

Figure 1(a) shows a radiation unit. This circularly polarized element consists of two closely spaced inclined radiating slots, perpendicular to each other and cut on an (Substrate Integrated Waveguide) SIW. Figure 1(b) shows the equivalent (Rectangular Waveguide) RWG antenna. Analyzing the equivalent RWG antenna instead of the SIW antenna allows reducing the simulation and analysis times. After the analysis process, the results must be transformed to be adapted for the synthesis of a SIW array.

A series of simulations based on a finite element method (HFSS14 software) were carried out for the characterization of the equivalent RWG radiating element. The waveguide is designed at 60 GHz using a Rogers RT=Duroid 6002 substrate ($\varepsilon_r = 2.94$) with a thickness of $b = 30$ mil. Here it should be

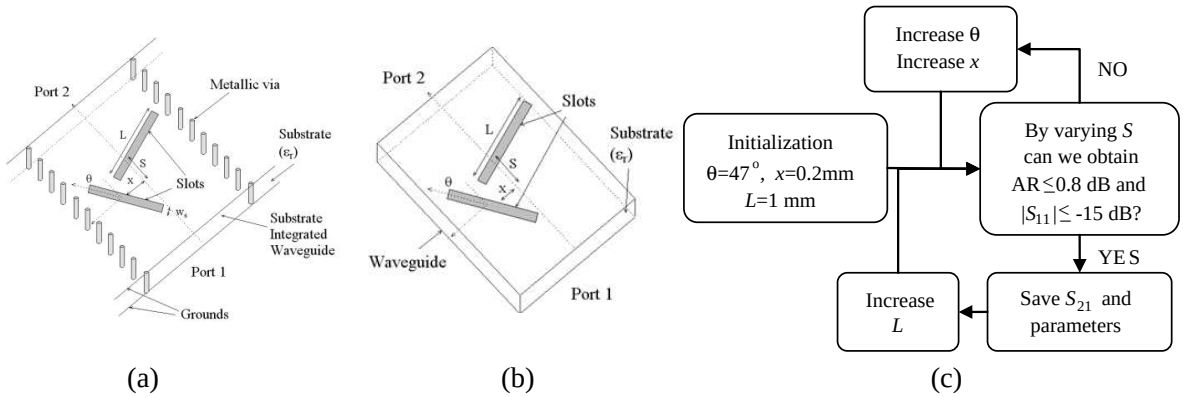

Figure 1. (a) Antenna element composed of two inclined slots on a SIW. (b) Classical rectangular waveguide model. (c) Algorithm for characterizing double slots element.

noted that the thickness has been chosen sufficiently high in order for an antenna element to be able to reach high maximum radiation. The waveguide has a width of $a = 2.43\,\text{mm}$.

The optimization procedure is outlined in Figure 2.

The parameters of the double inclined radiating slots, as shown in Figure 1(b), were varied in order to obtain a large range of values for the transmission coefficient $|S_{21}|$. For each obtained value of $|S_{21}|$, the radiating element must have a good performance in terms of circular polarization and return loss. The Axial Ratio requirement (AR < 0.8) is fulfilled by a proper choice of the spacing S, and the element excitation is controlled by the length (L) and the width (w_s) of the slots. The starting point for x must be chosen so that for each L in the range of interest, the slots do not overlap and remain inside the waveguide borders. In our simulations, it was not possible to obtain $|S_{21}|$ smaller than 0.6 due to the limitation of the length L. However, as it will be shown later in the paper, the obtained range for $|S_{21}|$ is enough for our array synthesis.

After completing the optimization procedure for the single elements, one can see in Figure 2(a) the magnitude of the transmission coefficient as a function of the slot length L, for different values of w_s,

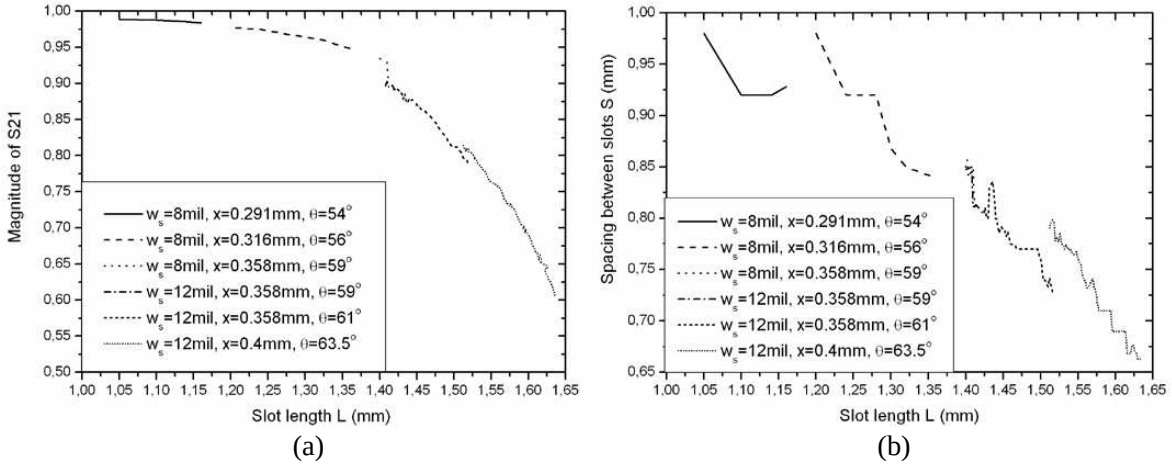

Figure 2. (a) Magnitude of $|S_{21}|$ versus length L for different parameters (w_s, x and θ) of optimized slots. (b) Spacing between slots versus length L for different parameters (w_s, x and θ) of optimized slots.

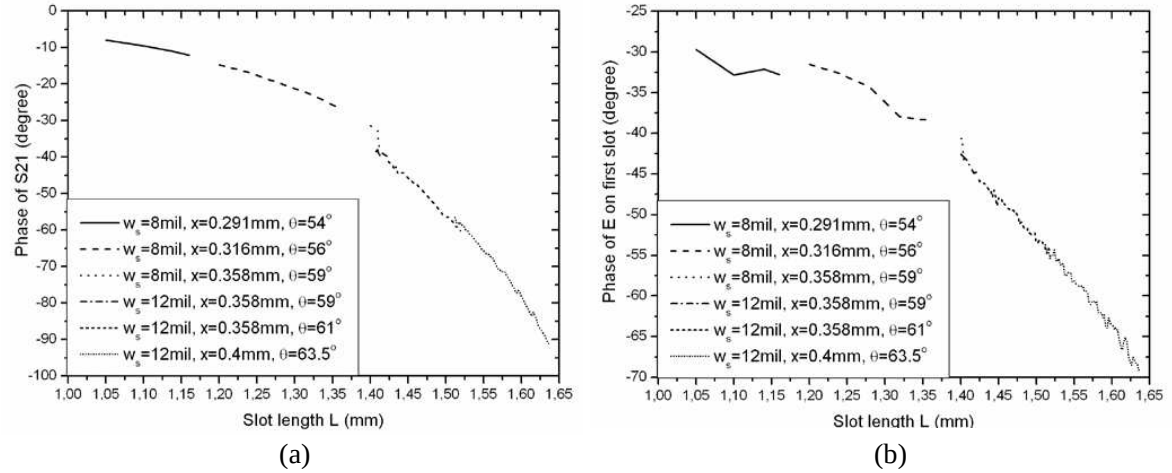

Figure 3. (a) Phase of S_{21} versus length L for different parameters (w_s, x and θ) of optimized slots. (b) Phase of the electric field on the first slot versus length L for different parameters (w_s, x and θ) of optimized slots.

θ, and x. It is possible to obtain value of $|S_{21}|$ ranging between 0.6 and 0.99. The spacing S versus the length L is shown in Figure 2(b), whereas Figures 3(a) and (b) present the phase of S_{21} and the phase of the electric field on the first slot, respectively. The phase of the electric field on the first slot is calculated at the position within the slot that gives the maximum amplitude of the electric field. The results in Figures 3(a) and (b) are required for determining the spacing between the array elements. It should be noted than more than 120 simulations were carried out for the characterization part.

3. SIW ARRAY SYNTHESIS

For the design of a travelling-wave linear array with a given distribution, it is possible to calculate the value of $|S_{21}|$ for each element of the array. Table 1 shows the required value of $|S_{21}|$ for each element of a 15-element array with different aperture distributions. Then, it will be possible to compare the performance in terms of efficiency of these 15-element arrays with the array designed in [19, 20] at 7.5 GHz. In Table 1, the values indicated in bold Italic cannot be reached by using the radiating element characterized in the previous subsection. From this, in our design, we consider that the last array elements are repeated by using the last feasible element. According to Table 1, the binomial aperture distribution has 5 non feasible elements. Thus, the binomial distribution was not designed.

For broadside radiation, the array elements should have an equiphase excitation. Thus, the distance between element n and element $n-1(D_n)$ must correspond to a full guided wavelength (λ_g) multiplied by a correction factor which takes into account the phase of the transmission coefficient of element $n-1$ (φ_{n-1}), and the difference between the phases of the electric fields on elements n and $n-1$ ($\Delta\alpha_n$). The distance D_n can be written as follows:

$$D_n = \lambda_g \left(1 + \frac{\varphi_{n-1}}{2\pi} + \frac{\Delta\alpha_n}{2\pi}\right) \tag{1}$$

Table A1 in the Annex presents the dimensions of a 60 GHz array with 15 elements and Taylor distribution. The phase parameters and the axial ratio of each array element are also reported in this table. The radiating elements were characterized for operating at 60 GHz, but the design dimensions were changed by using adequate translation factors for the designs of other antennas presented in this paper and operating at 77 GHz. From this, it is not necessary to repeat the characterization made at 60 GHz for designing the 77 GHz arrays.

Table 1. $|S_{21}|$ parameter for the different elements of the arrays.

$\|S_{21}\|$ for the different elements	**Distributions**			
	Uniform	**Tchebychev**	**Binomial**	**Taylor**
$\|S_{21}\|$ (1)	0.9375	0.9981	0.9999	0.992
$\|S_{21}\|$ (2)	0.9333	0.9888	0.999	0.983
$\|S_{21}\|$ (3)	0.9286	0.9672	0.9948	0.969
$\|S_{21}\|$ (4)	0.9231	0.9364	0.9817	0.952
$\|S_{21}\|$ (5)	0.9167	0.9047	0.9516	0.931
$\|S_{21}\|$ (6)	0.9091	0.8778	0.8983	0.906
$\|S_{21}\|$ (7)	0.9000	0.8534	0.8221	0.879
$\|S_{21}\|$ (8)	0.8889	0.8254	0.7294	0.847
$\|S_{21}\|$ (9)	0.8750	0.7884	0.6291	0.813
$\|S_{21}\|$ (10)	0.8571	0.7359	**0.5283**	0.773
$\|S_{21}\|$ (11)	0.8333	0.6594	**0.4317**	0.729
$\|S_{21}\|$ (12)	0.8000	**0.5549**	**0.3418**	0.678
$\|S_{21}\|$ (13)	0.7500	**0.4278**	**0.2595**	0.624
$\|S_{21}\|$ (14)	0.6667	**0.2876**	**0.1847**	**0.552**
$\|S_{21}\|$ (15)	**0.5000**	**0.1428**	**0.1169**	**0.529**

Once the rectangular waveguide arrays are designed, it is necessary to apply modifications to obtain the equivalent SIW arrays. This is done by taking into account the changes in the propagation constant and the radiation loss of the SIW. Indeed, SIWs and RWGs have different propagation constants, called $\beta_{g,\mathrm{SIW}}$ and $\beta_{g,\mathrm{RWG}}$. This difference must be taken into account for determining the distance between the elements in the SIW array. The relation between the distances D_n calculated for RWG arrays and those of SIW arrays can be written as:

$$D_{n,\mathrm{SIW}} = \frac{\beta_{g,\mathrm{RWG}}}{\beta_{g,\mathrm{SIW}}} D_{n,\mathrm{RWG}} \tag{2}$$

where the propagation constants $\beta_{g,\mathrm{RWG}}$ and $\beta_{g,\mathrm{SIW}}$ were calculated numerically (using HFSS simulator).

P_{SIW} and P_{RWG} are the power distributions in an SIW and its equivalent rectangular waveguide, respectively. To obtain the equivalent SIW array from our optimized RWG array, we must also take into account the relationship between P_{SIW} and P_{RWG} as follows:

$$P_{\mathrm{SIW}}(z_n) = P_{\mathrm{RWG}}(z_n) e^{-2\alpha z_n} \tag{3}$$

where α is the radiation loss constant and z_n is the position of element n of the array

$$z_n = \sum_{i=1}^{n} D_n \tag{4}$$

The radiation loss constant α of the SIW is calculated numerically. The parameters of each radiating element in the SIW array are modified to satisfy the required aperture power distribution (uniform, Tchebychev or Taylor distributions).

In a travelling-wave antenna, each element radiates a portion of the incident power and the leftover passes to the next radiating element. As it is impossible for the last element to radiate 100% power, in order to have no reflection, the antenna can be terminated in a matching load. However, short circuit terminations were enough for the 60 GHz and 77 GHz arrays since the residual power reaching the termination was less than 5% for these two antennas.

4. DESIGN OF THE SIWS

In the design of the SIW, the metallic via dimensions and the period must be chosen such that the TE_{10} mode exists but not the TE_{20} mode. It is also important to have low radiating loss. According to [6], for an SIW made with metallic cylinders of diameter d and with period p, these conditions are achieved when the design parameters fit with the following:

$$p > d \tag{5}$$

$$\frac{p}{\lambda_c} < 0.25 \tag{6}$$

4.1. SIW at 60 GHz

The dimensions of an SIW made with metallic cylinders were optimized for operating at 60 GHz. a, b, and ε_r are respectively the waveguide width, the substrate thickness, and the substrate permittivity. The following are the optimized parameters: $a = 2.43$ mm, $b = 0.762$ mm, $p = 1.4$ mm, and $d = 0.81$ mm, and $\varepsilon_r = 2.94$. With these parameters, the cutoff frequency of the TE_{10} mode, $f_{cTE_{10}}$, is around 40 GHz and the cutoff frequency of the TE_{20} mode is around 75 GHz. A quasi-linear behavior of the propagation constant was observed in the frequency band from $1.2 \times f_{cTE_{10}}$ to $1.9 \times f_{cTE_{10}}$. A component working in this frequency band will suffer less from dispersion and may have larger frequency bandwidth.

4.2. SIW at 77 GHz

The same procedure was done for an SIW operating at 77 GHz. The optimized dimensions are $a = 2.43$ mm, $b = 0.508$ mm, $p = 1.4$ mm and $d = 1.24$ mm. For these dimensions, the cutoff frequencies of the TE_{10} and TE_{20} modes are 49 GHz and 98 GHz, respectively. Again, the frequency of 77 GHz is located in the center of the frequency bandwidth with a quasi-linear behavior of the propagation constant.

5. DESIGN OF THE TRANSITIONS

This section presents the design of transitions between an SIW and connectors used for measurements.

5.1. Transition at 60 GHz

A WR15/SIW transition as shown in Figure 4 has been designed for the antenna operating at 60 GHz. The optimized transition gives a return loss less than −10 dB in the band 55 GHz–65 GHz.

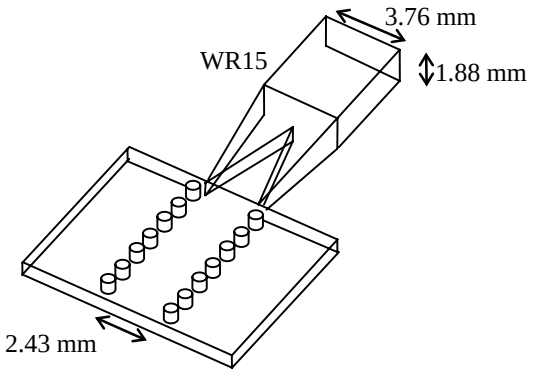

Figure 4. WR15/SIW optimized transition at 60 GHz.

5.2. Transition at 77 GHz

A WR10/SIW transition developed at the Poly-Grames research center has been used for the antennas operating at 77 GHz.

6. NUMERICAL RESULTS

Simulations that follow were performed with Ansoft HFSS. Return losses and axial ratios of the designed 60 GHz arrays are plotted in Figures 5(a) and (b). These results show that the operating bandwidths are fixed by the axial ratio curves. The obtained gains in the broadside direction are plotted in Figure 5(c). The realized gain takes into account the power reflected at the input array port as well as the dielectric losses. Figures 6(a)–(c) show the computed results for the 77 GHz arrays.

The radiating features of the designed arrays 60 GHz and 77 GHz are summarized in Table 2. In this table, the best performances are indicated in bold. From these results, the lower side lobe

Table 2. performances for antennas operating at 60 and 77 GHz.

Operating frequency	Performances	Distributions		
		Uniform	**Tchebychev**	**Taylor**
60 GHz	**Gain**	**16.73 dB**	16.23 dB	16.47 dB
	AR	1.06 dB	1.53 dB	**0.06 dB**
	$\|S_{11}\|$	**−15.2 dB**	−13.5 dB	−13.5 dB
	SLL	−17 dB	−25 dB	**−26.6 dB**
77 GHz	**Gain**	16.2 dB	15.7 dB	**16.7 dB**
	AR	**0.94 dB**	2.2 dB	1.7 dB
	$\|S_{11}\|$	**−15.5 dB**	−15.3 dB	−15.1 dB
	SLL	−14.8 dB	−23.5 dB	**−25.8 dB**

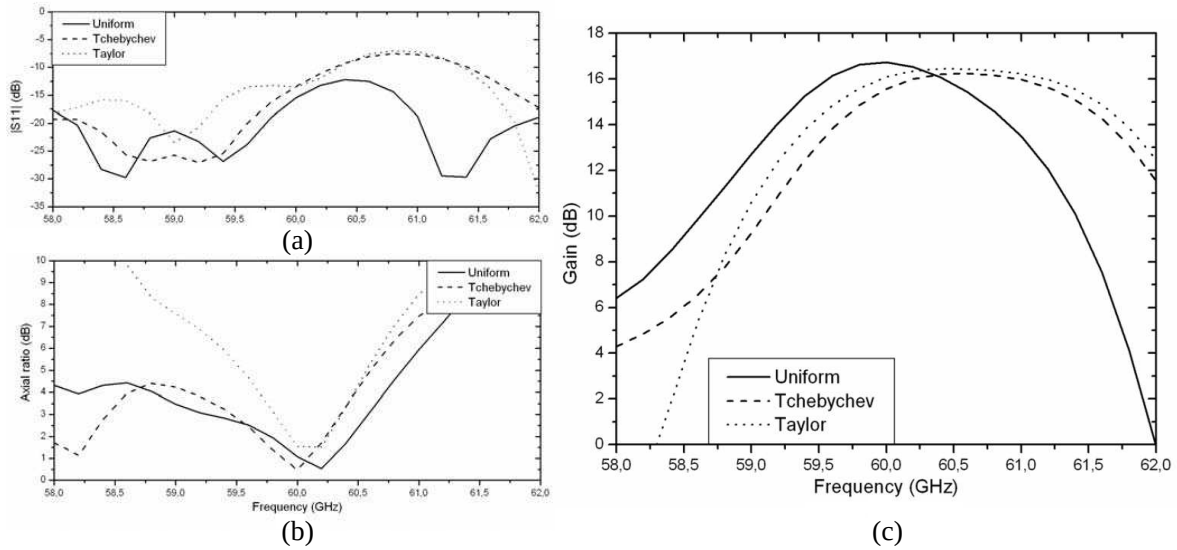

Figure 5. Antennas operating at 60 GHz: (a) simulated return loss, (b) axial ratio at broadside direction, and (c) gain at broadside direction versus frequency for different aperture distributions.

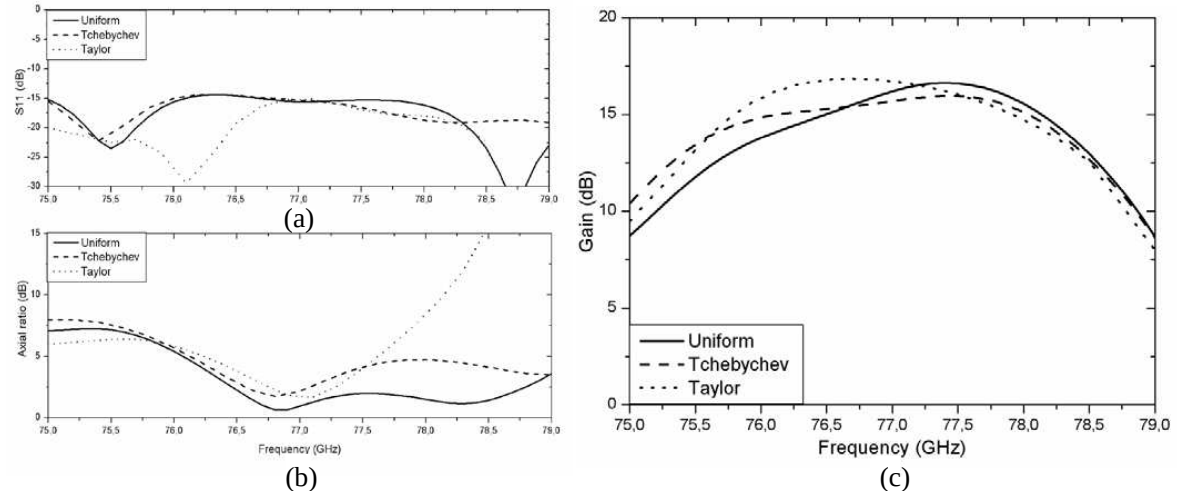

Figure 6. Antennas operating at 77 GHz: (a) simulated return loss, (b) axial ratio at broadside direction, and (c) gain at broadside direction versus frequency for different aperture distributions.

level is obtained with the Tchebychev or Taylor aperture distributions, as expected. Furthermore, the optimized antennas with Taylor distribution give a better compromise for low side lobes and good circular polarization. This is probably due to the fact that arrays with Taylor distribution are easier to design than those with the Tchebychev distribution, as this can be deducted from Table 1. Indeed, Table 1 shows that it is easier to achieve the design rules for the Taylor distribution since fewer number of required values of $|S_{21}|$ are unfeasible.

It should be noted that for all the designed 15-element arrays the obtain radiation efficiency is about 78%, whereas it is more than 90% for a similar antenna array operating 7.5 GHz as proposed in [19, 20]. This is due to the increase of the radiation loss at millimeter waves and the higher dielectric loss of the substrate material that is used here. To increase the radiation efficiency other better material should be used.

7. EXPERIMENTAL RESULTS

To validate the proposed analysis, arrays operating at 77 GHz were fabricated. Figure 7 shows a photo of the prototype array with uniform distribution. The measured and simulated return losses for uniform and Taylor distributions are plotted in Figure 8, showing that a good impedance matching is obtained with the fabricated antennas.

The measured axial ratios are reported in Figure 8(b), showing that, at 77 GHz, a better circular polarization characteristic is obtained for the antenna with uniform distribution.

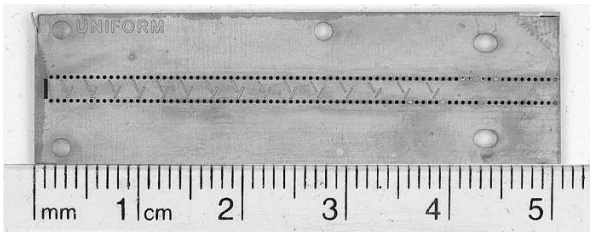

Figure 7. Photo of a fabricated 77 GHz array antenna.

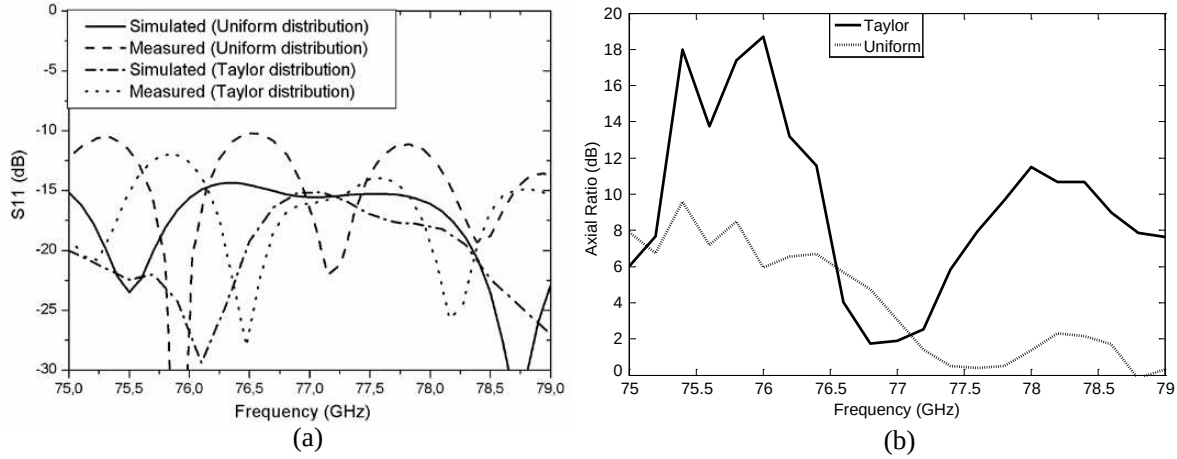

Figure 8. (a) Measured return loss, (b) measured axial ratio.

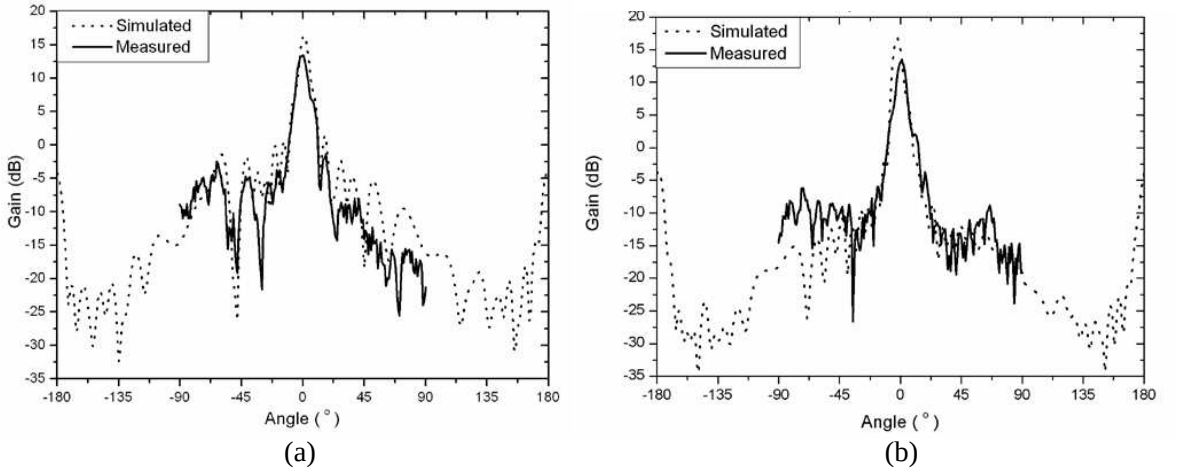

Figure 9. Simulated and measured radiation patterns at 77 GHz: (a) for uniform distribution, (b) for Taylor distribution.

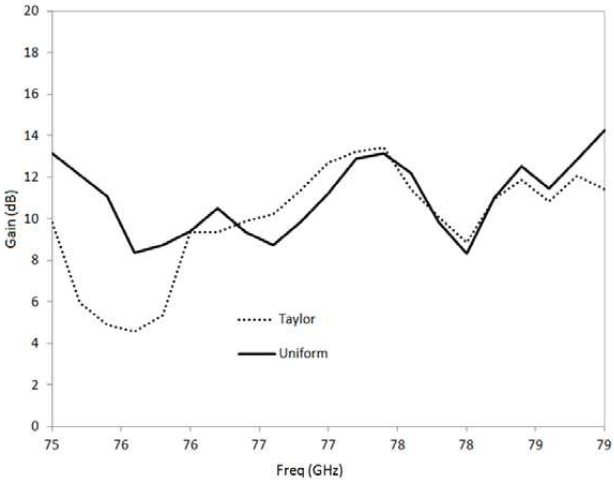

Figure 10. Measured gain at broadside direction versus frequency for Taylor and uniform distributions.

Experimental as well as numerical results for the radiation pattern are plotted in Figures 9(a) and (b), for uniform and Taylor distributions, respectively. A good agreement is obtained between the simulated and measured results. The measured gain versus frequency is shown in Figure 10. The discrepancies between simulated and experimental results, in particular, the observed lower gains in the fabricated antennas compared to the simulated results are probably due to tolerance in the dielectric constant of the substrate, the tolerances in the fabrication and the tolerance in the antenna alignment during measurement.

8. CONCLUSION

This paper has presented the analysis and synthesis of millimeter-wave substrate integrated travelling-wave linear antenna arrays with circular polarization. Antenna arrays with different power distributions, including the transitions and terminations, are analyzed and designed for communication and radar systems at 60 GHz and 77 GHz.

Full-wave simulation results show that the optimized antennas present good performances in terms of impedance matching, gain and axial ratio. The design method allows the control of the main beam's orientation, gain and side lobe levels. Furthermore, experimental results were presented to validate the proposed designs and techniques. It should be noted that the gain can be increased by using a power divider and several linear arrays. Indeed, gains above 30 dB are required in radar applications.

ACKNOWLEDGMENT

The authors wish to thank Ms. Hoda Nematollahi and the technicians of Poly-Grames research centre. The authors wish also to thank NSERC, FQRNT and *Centre de Recherche En Electronique Radiofréquence* (CREER).

APPENDIX A.

Table A1. 60 GHz Array dimensions for 15 elements with Taylor distribution.

#	W (mil)	X (mm)	θ (°)	L (mm)	S (mm)	$\lvert S_{21}\rvert$	$\varphi_{S_{21}}$ (°)	φ_E (°)	S_{11} (dB)	AR (dB)
1	8	0.291	54	1.05	0.98	0.99	−8	−29.6	−29	0.4
2	8	0.291	54	1.16	0.92	0.98	−12	−32.8	−29	0.2

#	W (mil)	X (mm)	θ (°)	L (mm)	S (mm)	$\lvert S_{21}\rvert$	$\varphi_{S_{21}}$ (°)	φ_E (°)	S_{11} (dB)	AR (dB)
3	8	0.316	56	1.28	0.92	0.97	−20	−34.3	−23	0.2
4	8	0.316	56	1.36	0.83	0.95	−27	−38.4	−24	0.2
5	8	0.358	59	1.402	0.85	0.93	−32	−40.6	−21	0.5
6	12	0.358	59	1.4	0.85	0.90	−37	−42.5	−18	0.1
7	12	0.358	61	1.44	0.79	0.88	−44	−47.1	−19	0.5
8	12	0.358	61	1.474	0.77	0.85	−50	−49.8	−19	0.3
9	12	0.358	61	1.498	0.76	0.81	−56	−52.2	−17	0.4
10	12	0.4	63.5	1.544	0.76	0.77	−64	−57.1	−16	0.6
11	12	0.4	63.5	1.58	0.71	0.73	−72	−60.6	−17	0.4
12	12	0.4	63.5	1.605	0.69	0.68	−80	−63.9	−16	0.1
13	12	0.4	63.5	1.63	0.66	0.63	−88	−67.9	−16	0.7
14	12	0.4	63.5	1.636	0.66	0.55	−91	−69.2	−17	0.8
15	12	0.4	63.5	1.636	0.66	0.52	−91	−69.2	−17	0.8

REFERENCES

1. Yang, J., G. Pyo, C.-Y. Y. Kim, and S. Hong, "A 24-GHz CMOS UWB radar transmitter with compressed pulses," *IEEE Trans. Microw. Theory Tech.*, Vol. 60, No. 4, 1117–1125, 2012.
2. Lee, S., S. Kong, C.-Y.. Kim, and S. Hong, "A low-power K-band CMOS UWB radar transceiver IC for short range detection," *Proc. IEEE Radio Frequ. Integra. Circuits Symp.*, 503–506, Daejeon, South Korea, 2012.
3. Hasch, J., E. E. Topak, R. Schnabel, T. Zwick, R. Weigel, and C. Waldschmidt, "Millimeter-wave technology for automotive radar sensors in the 77 GHz frequency band," *IEEE Trans. Microw. Theory Tech.*, Vol. 60, No. 4, 845–860, 2012.
4. Fisher, A., A. Stelzer, and L. Maurer, "A 77-GHz antenna and fully integrated radar transceiver in package," *IEEE International Journal of Microwave and Wireless Technologies*, Vol. 4, 447–453, 2012.
5. Perahia, E., C. Cordeiro, M. Park, and L. L. Yang, "IEEE 802.11ad: Defining the next generation multi-Gbps wi-fi," *Proceedings IEEE Consumer Communications and Networking Conference (CCNC)*, 1–5, Hillsboro, USA, 2010.
6. Bozzi, M., A. Georgiadis, and K. Wu, "Review of substrate-integrated waveguide circuits and antennas," *IET Microwaves, Antennas & Propagation*, Vol. 5, No. 8, 909–920, 2011.
7. El Mostrah, A., B. Potelon, E. Rius, C. Quendi, J. Favennec, and H. Leblond, "Comparative study of two C-band SIW filter topologies for a space application," *Proc. European Microwave Conference (EuMC)*, 368–371, Brest, France, 2012.
8. Lian, W. and W. Hong, "Substrate integrated coaxial line 3 dB coupler," *Electronics Letters*, Vol. 48, No. 1, 35–36, 2012.
9. Djerafi, T., J. Gauthier, and K. Wu, "Variable coupler for Butler beam-forming matrix with low sidelobe level," *IET Microwaves, Antennas & Propagation,* Vol. 6, No. 9, 1034–1039, 2012.
10. Djerafi, T., M. Daigle, H. Boutayeb, X. P. Zhang, and K. Wu, "Substrate integrated waveguide six-port broadband front-end circuit for millimeter-wave radio and radar systems," *Proc. European Microwave Conference (EuMC)*, 77–80, Roma, Italy, 2009
11. Liu, J. H., D. R. Jackson, and Y.-L. L. Lon, "Substrate integrated waveguide (SIW) leaky-wave antenna with transverse slots," *IEEE Trans. Antennas Propag.*, Vol. 60, No. 1, 20–29, 2012.
12. Chen, J.-X. X., W. Hong, Z. Hao, P. Yan, X. Zhu, J.-Y. Y. Zhou, C. Peng, and K. Wu, "Development of a single board microwave sub-system based on substrate integrated waveguide (SIW) technology," *Proc. IEEE Microwave Symposium Digest (MTT)*, 1–3, Montreal, Canada, 2012.

13. Li, Z. and K. Wu, "24-GHz frequency-modulation continuous-wave radar front-end system-on-substrate," *IEEE Trans. Microw. Theory Tech.*, Vol. 56, No. 2, 278–285, 2008.
14. Han, L. and K. Wu, "24-GHz integrated radio and radar system capable of time-agile wireless communication and sensing," *IEEE Trans. Microw. Theory Tech.*, Vol. 60, No. 3, 619–631, 2012.
15. Nematollahi, H., H. Boutayeb, and K. Wu, "Mm-wave circularly polarized SIW traveling-wave antennas," *Proc. European Microwave Conference (EuMC)*, Roma, Italy, 2009.
16. Zhang, Q. F. and Y. L. Lu, "45° linearly polarized substrate integrated waveguide-fed slot array antennas," *Proc. IEEE Microwave and Millimeter Wave Technology (ICMMT)*, Vol. 3, 1214–1217, Nanjing, China, 2008.
17. Peters, F. D., S. O. Tatu, and T. Denidni, "Design of beamforming slot antenna arrays using substrate integrated waveguide," *Proc. IEEE Antennas and Propag. Society Intern Symp. (APSURSI)*, 1–2, Spokane, USA, 2011.
18. Chen, P., W. Hong, Z. Kuai, and J. Xu, "A substrate integrated waveguide circular polarized slot radiator and its linear array," *IEEE Antennas Wireless Propag. Lett.*, Vol. 8, 1536–1225, 2009.
19. Montisci, G., "Design of circularly polarized waveguide slot linear arrays," *IEEE Trans. Antennas Propag.*, Vol. 54, No. 10, 3025–3029, Oct. 2006.
20. Montisci, G., M. Musa, and G. Mazzarella, "Waveguide slot antennas form circularly polarized radiated field," *IEEE Trans. Antennas Propag.*, Vol. 52, No. 2, 619–623, Feb. 2004.